The effect of localized deformation on the indentation crack growth in Si_3N_4

Z. Iždinská[1]*, Z. Gábrišová[1], E. Gondár[1], M. Zemánková[2]

[1] *Institute of Technologies and Materials, STU, Pionierska 15, 831 02 Bratislava, Slovak Republic*
[2] *Institute of Materials and Machine Mechanics, SAV, Račianska 75, 831 02 Bratislava, Slovak Republic*

Received 9 January 2009, received in revised form 30 March 2009, accepted 14 April 2009

Abstract

The effect of additional deformation on crack growth resistance by mechanical (bending) and cyclic thermal loading on silicon nitride specimens was investigated. Cracks initiated primarily by Vickers indenter were formed in the corners of impression. Secondary impressions induced localized deformation at the crack tips. The influence of introduced deformation on indentation crack growth was not the same for bending and thermal cycling. Localized deformation resulted in the half of the specimens in small increase, and in the other half in small degradation of the fracture forces during mechanical loading. In contrary, the suppression of the indentation crack growth was observed in 80 % of the specimens after thermal cycling. The ambiguity of attained results can be explained by the interaction of primary and secondary indentation cracks. The effect of localized deformation on the suppression of indentation crack growth overlaps with the effect of secondary cracks formation.

Key words: Si_3N_4, deformation, bending testing

1. Introduction

Silicon nitride is significant representative of structural ceramics for applications in high temperature conditions [1, 2]. In these conditions internal stresses are intensively generated mainly due to repeated thermal shocks, resulting into the growth of existing cracks. This may lead to the component failure after certain number of thermal cycles [3]. High temperature properties are most frequently characterized by creep tests [4, 5]. The most widely spread thermal shocks resistance test is indentation-cooling test [6]. The principle of this test is based on heating of specimen with the crack and its subsequent rapid cooling in cooling media container. Rapid heating (laser, electron beam) allows speeding up testing procedure [7, 8]. Replacement of cooling container by new apparatuses (water jet system) leads to intense thermal shock loading [9].

The main disadvantage of silicon nitride as well as structural ceramics in general is their brittleness. Great effort has been devoted to the understanding of the process of crack initiation and growth in ceramic materials. Processes directed to the formation of so called processed zone at the crack tip that lead to the increase of fracture toughness via employment of various toughening mechanisms [5, 10] have been investigated. Indeed ceramic materials based on Si_3N_4 and Al_2O_3 exhibit crack growth resistance increase with the growth of crack length that is called R-curved behaviour.

Due to favourable mechanical properties, composite materials like Si_3N_4 + SiC particles have attracted attention. Toughening of ceramic materials by whiskers appears as very promising. Systems including $Al_2O_3 + SiC_w$, $Si_3N_4 + SiC_w$, Si_3N_4 + β-Si_3N_{4w}, and SiC_w are of primary interest.

Fracture toughness in the system Si_3N_4 + β-Si_3N_{4w} increases due to mechanism of crack buckling and whisker-matrix interface debonding. The mechanism of fibre pulling appeared very rarely, particularly in case of very short whiskers [12].

Another possibility of increasing ceramic materials toughness is the employment of transformation mechanisms in a process zone in front of the crack, that take place in the systems with ZrO_2, TiC, or TiB_2

*Corresponding author: tel.: +421 2 44455087-377; fax: +421 2 44455086; e-mail address: zita.izdinska@stuba.sk

(e.g. $Al_2O_3 + ZrO_2$, $SiC + TiC$, $Si_3N_4 + ZrO_2$). Crystallographic transformation accompanied by volume increase (3–5) % occurs in the case of ZrO_2 ceramics due to high tensile stresses or temperatures (950–1150) °C. Transformation causes formation of compression stresses at the tip of the growing crack. Additional energy is needed for further growth of the crack [13]. At temperatures over 1300 °C, the drop of crack growth rate dependence on stress intensity factor was determined during cyclic bending of Si_3N_4 [14]. This contradiction with the conventional knowledge (Paris law) most probably results from the softening around elongated grains of the binding phase. These get elongated due to tensile stress at high temperature and hinder the grain growth. Two possible hindering modes of crack growth are assumed. The first is crack transition through softened grain and the second is crack loop creation round the grain.

The aim of this paper is to examine the influence of additional very localized deformation on indentation crack growth resistance during mechanical and cyclic thermal loading in silicon nitride. Additional deformation will induce compression stresses at the tip of existing Vickers indentation cracks and so retard further growth of the crack. Silicon nitride deformation due to mechanical loading was characterized in previous contributions [15, 16].

2. Experiment

Si_3N_4 (mass ratio 85.36 wt.%) with activating additives Al_2O_3 (4.3 wt.%) and Y_2O_3 (10.34 wt.%) was used as an experimental material. This mass ratio corresponds to 10 % YAG. Silicon nitride specimens were prepared by cold pressing and subsequent hot pressing in nitrogen atmosphere [17], under the following conditions: $T = 1680$ °C, $t = 20$ min, $p = 30$ MPa. Average density was 3.271 g cm^{-3}, which corresponds to 97.92 % theoretical density.

In total, 32 specimens of circular cross section with the diameter 8 mm were prepared and Vickers hardness and indentation fracture toughness were determined [18]. The thickness of each specimen is given in Table 1. The average hardness value was (15862 ± 176) MPa and fracture toughness was (5.61 ± 0.10) MPa m$^{1/2}$.

Specimens were gathered into 16 couples with equal hardness and fracture toughness. The difference in fracture toughness values within a couple did not exceed 2.9 %. Primary impressions were initiated by Vickers indenter with the loading force $F_p = 294.3$ N in the middle of each specimen. The tips of the indentation cracks were deformed locally by secondary impression using Rockwell indenter and the loading force $F_s = 202.3$ N (Fig. 1). Rockwell indenter was chosen to prevent additional crack formation in the corners of impression as it was by Vickers indenter.

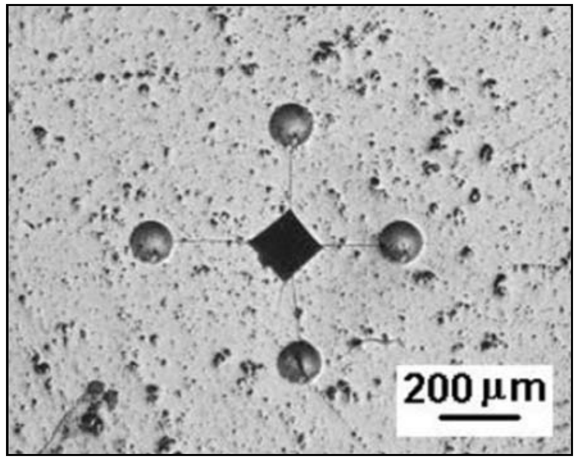

Fig. 1. Specimen with the primary Vickers indent and indentation cracks and secondary impressions by Rockwell ball causing very localized deformation at the original crack tips.

The influence of such localized deformation on the indentation initiated cracks growth resistance was examined by mechanical and cyclic thermal loading.

Six specimen couples were loaded mechanically in bending in a specially designed fixture which assured that the fracture occurred from the primary indentation cracks (Fig. 2).

The groove (4) in the lower part of the fixture (5) was milled and in the middle of the groove a countersink (6) for specimen insert was prepared. The specimen with the indentation cracks at the tensile side was oriented in such a way that one diagonal of the indent and the corresponding indentation cracks were parallel to the longitudinal axis of the groove. The bending force was applied using a pin in the centre of the upper side of the specimen and opposite to the indent while the lower supports correspond to the edges of the groove. Loading rate of 1 mm min^{-1} was applied using 5 kN Along MESS equipment. Specimens were loaded to fracture until specimen fracture (Fig. 3).

Another 10 couples of specimens were used for the evaluation of influence of additional deformation on crack growth resistance due to cyclic thermal shock loading. A new cyclic thermal shocks testing method shown in Fig. 4 was applied [19, 20].

The specimen (1) with the indentation crack is heated and pushed by the punch (3) on a sealing (4). The punch is heated by an induction coil (6). The compression force of the punch (controlled by used weights) prevents the cooling water from leaking from under the sealing (4). The specimen is loaded in shear on perimeter of the punch, and by thermal stresses from cyclic thermal shocks on the surface. The employment of smaller diameter punch induces bending loading of the specimen. Cyclic thermal shocks

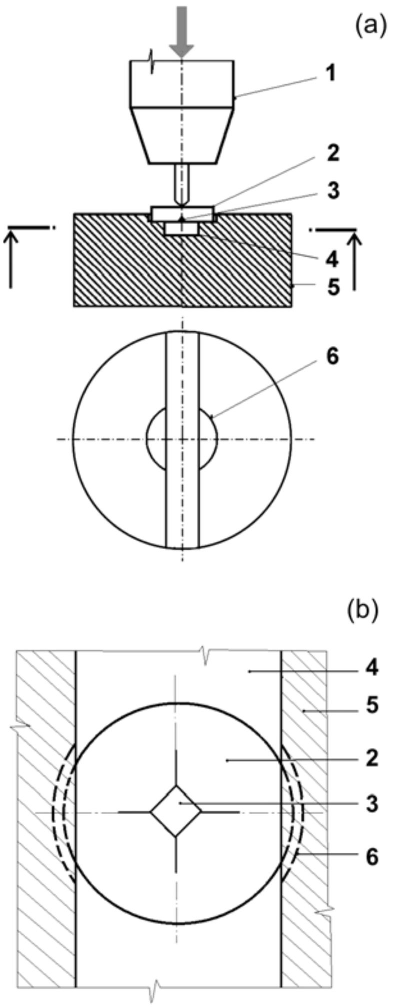

Fig. 2. The design of the fixture for the loading of the circular specimens in bending assures that the fracture occurs from the indentation cracks (a); (b) bottom view of the specimen with the indentation cracks orientation: 1 – moving element, 2 – specimen, 3 – impression, 4 – groove, 5 – static element, 6 – countersink.

were applied using following parameters [20]: $T_{\max} = 1100\,^{\circ}\mathrm{C}$, $T_{\min} = 500\,^{\circ}\mathrm{C}$, $t_{\max} = 16\,\mathrm{s}$, $t_{\min} = 6\,\mathrm{s}$, diameter of the punch ø 5 mm.

Individual specimens from couples were loaded by equal number of cycles, and the length of original indentation initiated cracks was measured. Number of cycles initiating the crack growth in specimens with primary impression was determined. Specimens with primary and secondary impressions were subjected to the same number of cycles. Propagation of initiated cracks was observed.

3. Results and discussion

Bending test yielded the relationship between the loading force and the deflection of the specimen until fracture. The relationship between the loading force and the deflection for the specimen couple No. 5 is documented in Fig. 5. These fracture forces were compared for each couple and the results are given in Table 1.

No straightforward effect of introduced deformation was determined. In the case of couples 4, 5 and 6, secondary impressions caused an increase of the fracture forces, however the forces increase was marginal. The highest increase in the couple No. 11 was 7.4 %; the lowest in the couple No. 6 was only 1.9 %.

An opposite effect was obtained for the specimen couples 1, 2 and 3, when additional Rockwell indents resulted in the reduction of the fracture forces. Fracture force degradation in couple No. 1 was 11 % and the smallest drop of 3.4 % was measured in the couple No. 2.

Negative influence of additional deformation on the

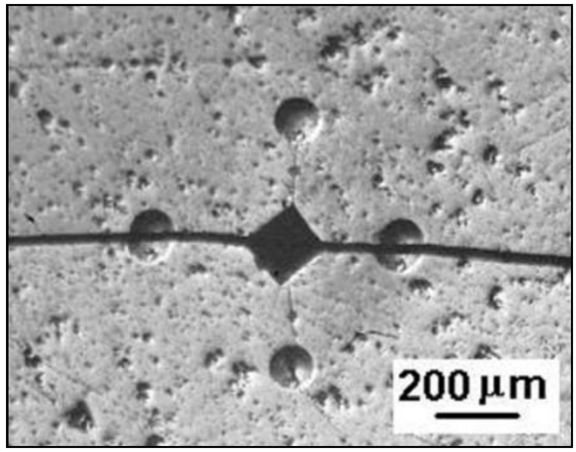

Fig. 3. Fractured specimen.

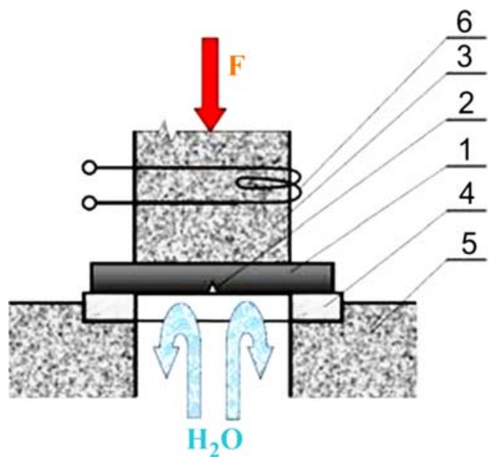

Fig. 4. The principle of cyclic thermal shocks testing method: 1 – specimen, 2 – impression, 3 – punch, 4 – sealing, 5 – support, 6 – inductor.

Table 1. The results of bending tests on the indented samples and indented samples with the additional local plastic deformation

Experimental material	Couple No.	Specimen thickness (mm)	Specimen No.	Type of impression	$F_{\max}$ (N)	ΔF (%)
Si_3N_4 + 10%YAG	1	2.1	1	HV	465.59	−11.4
			2	HV + HR	418.11	
	2	1.7	3	HV	324.06	−3.4
			4	HV + HR	313.34	
	3	2.1	5	HV	532.60	−10.1
			6	HV + HR	483.56	
	4	2.0	7	HV	402.53	4.0
			8	HV + HR	419.43	
	5	2.0	9	HV	359.83	7.4
			10	HV + HR	388.52	
	6	1.8	11	HV	337.49	1.9
			12	HV + HR	344.01	

Table 2. The effect of thermal cycling on the indentation crack growth

Couple No.	Specimen thickness (mm)	Specimen No.	Type of impression	Applied cycles	Result
7	2.1	13	HV	8	cracks growth
		14	HV + HR	8	cracks growth
8	1.7	15	HV	4	cracks growth
		16	HV + HR	4	cracks length unchanged
9	2.1	17	HV	4	cracks growth
		18	HV + HR	4	cracks length unchanged
10	2.0	19	HV	8	cracks growth
		20	HV + HR	8	cracks length unchanged
11	2.0	21	HV	4	cracks growth
		22	HV + HR	4	cracks length unchanged
12	1.8	23	HV	8	cracks growth
		24	HV + HR	8	cracks length unchanged
13	2.1	25	HV	4	cracks growth
		26	HV + HR	4	cracks growth
14	2.1	27	HV	4	cracks growth
		28	HV + HR	4	cracks length unchanged
15	2.0	29	HV	8	cracks growth
		30	HV + HR	8	cracks length unchanged
16	2.0	31	HV	4	cracks growth
		32	HV + HR	4	cracks length unchanged

fracture force can be explained based on Fig. 6. The deformed area under the primary impression (made by Vickers indenter) is much larger in comparison with the deformed area under the secondary (Rockwell) impression. Despite similar indentation force, the geometry of Vickers indenter enables better penetration

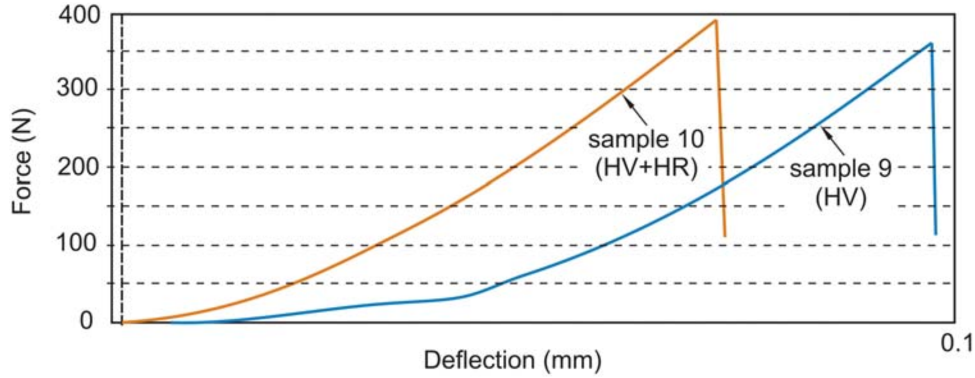

Fig. 5. Force vs. deflection for couple No. 5.

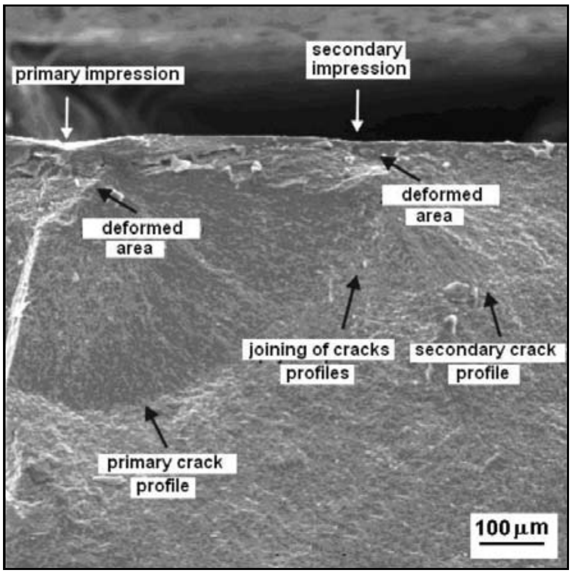

Fig. 6. Fracture surface detail, specimen No. 2, couple No. 7.

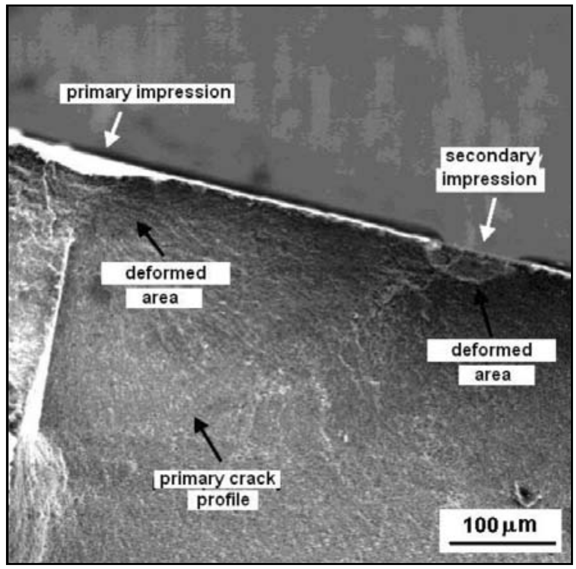

Fig. 7. Fracture surface detail, specimen No. 8, couple No. 10.

into the experimental material. This results in higher penetration depth, larger deformed area under the impression and larger indentation cracks than in the case of Rockwell indentation. Joining of crack profiles is visible on Fig. 6. Two cases are principally possible. Vickers and Rockwell indentation cracks either interact or they do not interact to form a larger crack. This can explain the degradation of the fracture force in the specimens No. 2, 4 and 6. In case of specimens No. 8, 10 and 12, secondary cracks did not interact with the primary cracks (Fig. 7), and the deformed area at the tip of the primary crack caused an increase in fracture force.

The effect of localized deformation on Vickers indentation cracks during cyclic thermal loading is summarized in Table 2.

The growth of the Vickers indentation cracks was observed in all samples after thermal cycling (Table 2). The effect is illustrated in Fig. 8. However, the length of the cracks with secondary Rockwell indents did not occur after identical loading (Fig. 9) except two cases, No. 7 and 13. Thus local indents resulted in 80 % in the increase of the resistance to crack growth under conditions of thermal cycling. The remaining 2 cases, when crack grew, can be explained in terms of the effect of Herzian cracks on the radial cracks from Vickers indentation similarly as in the specimen No. 2 in Fig. 6. Only in those cases when Herzian cracks are absent or oriented unfavourably to primary cracks, their interaction is missing and the localized deformation has favourable effect.

The load used for Rockwell indents had been obviously too high which resulted in the formation of Herzian cracks besides localized plastic deformation.

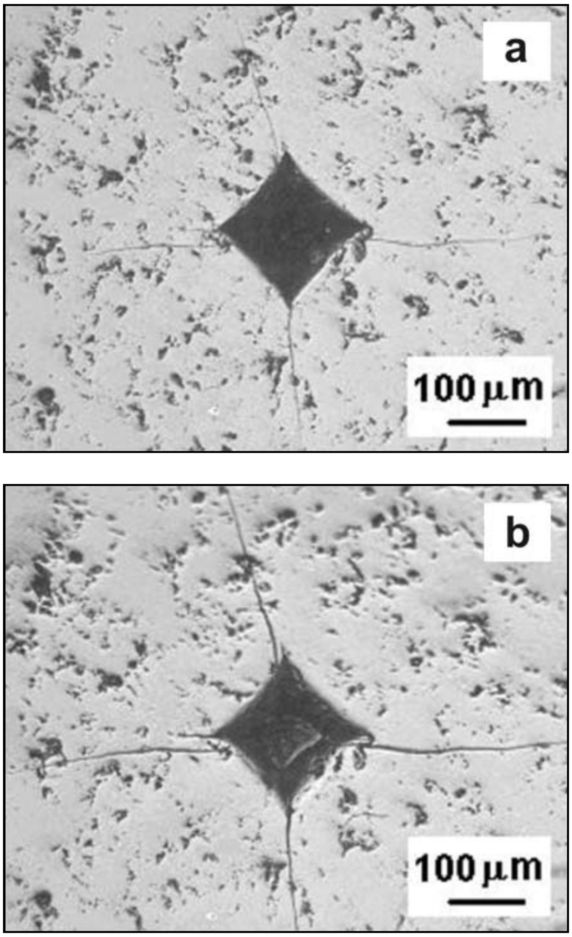

Fig. 8. Primary cracks growth by the specimen No. 19, couple No. 10: (a) initial state, (b) after 8 cycles.

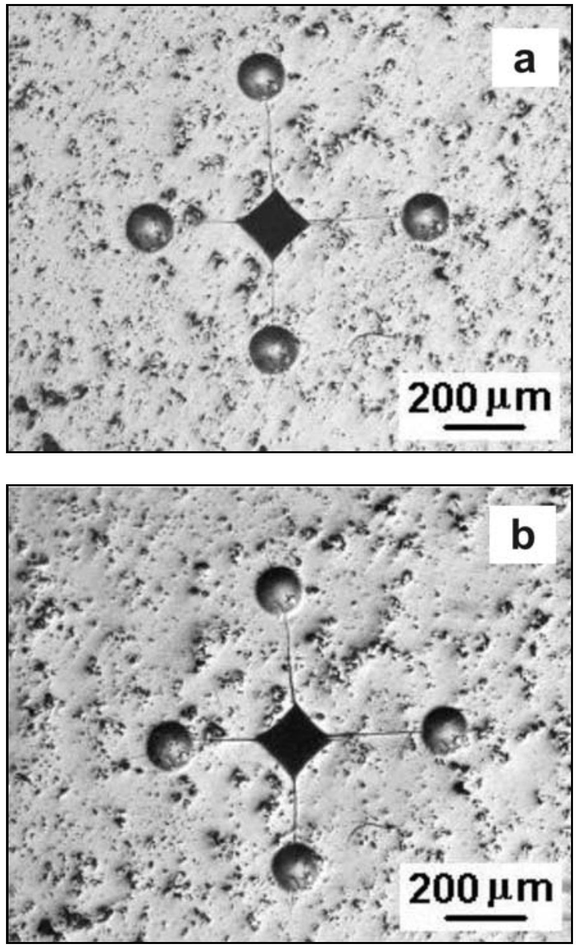

Fig. 9. Specimen with primary and secondary impressions, specimen No. 20, couple No. 10: (a) initial state, (b) after 8 cycles.

Positive effect of such localized deformation can be expected only in the case when secondary Herzian cracks do not form or they do not interact with primary cracks. Secondary crack formation depends on the particular indentation force. Certain level of loading force not yet leading to the formation of additional cracks can be assumed. The question is whether this loading is large enough to induce sufficiently large deformation necessary for crack growth retardation. Already in our case the deformed zone was relatively small. Another possibility how to prevent secondary cracks formation consists in the application of material with higher toughness. The preliminary determination of the orientation of secondary cracks not interacting with primary cracks is not possible.

4. Conclusion

The effect of localized plastic deformation on indentation crack growth is different for bending and thermal cycling.

Localized deformation resulted in the half of the specimens in small increase, and in the other half in small degradation of the fracture forces during mechanical loading.

In contrary, the suppression of the indentation crack growth was observed in 80 % of the specimens after thermal cycling.

The ambiguity of attained results can be explained by the interaction of primary and secondary indentation cracks. The effect of localized deformation on the suppression of indentation crack growth overlaps with the effect of secondary crack formation.

It is necessary to find out such level of secondary Rockwell indentation force that will result in sufficient size of deformed cracks free zone formation.

Acknowledgements

The support of a grant VEGA1/4094/07 from Ministry of Education of Slovak Republic is gratefully acknowledged.

References

[1] HVIZDOŠ, P.—LOFAJ, F.—DUSZA, J.: Kovove Mater., *33*, 1995, p. 473.

[2] HVIZDOŠ, P.—KAŠIAROVÁ, M.—DUSZA, J.—HNATKO, M.—ŠAJGALÍK, P.: Kovove Mater., *42*, 2004, p. 51.

[3] CLAUSSEN, N.—HASSELMAN, D. P. H.: Thermal Stresses in Severe Environments. New York, Plenum Press 1992.

[4] LUBE, T.—DUSZA, J.: J. Eur. Ceram. Soc., *27*, 2007, p. 1203.

[5] KOVALČÍK, J.: Vysokoteplotné vlastnosti konštrukčných keramických materiálov na báze Si_3N_4. [Dizertačná práca]. Košice, ÚMV SAV 2003.

[6] CRANDALL, W. B.—GING, J.: J. Am. Ceram. Soc., *38*, 1995, p. 44.

[7] SCHAUS, M.—POHL, M.: Metall., *5*, 1998, p. 464.

[8] KADNER, J.—MENZEL, S.—WETZIG, K.: Fresenius J. Anal. Chem., *361*, 1998, p. 578.

[9] ABSI, J.—GLANDUS, J. C.: In: J. Euro. Ceram. Soc., *24*, 2003, p. 2835.

[10] KALANTAR, M.—FANTOZZI, G.: Mat. Sci. and Eng. A, *472*, 2008, p. 273.

[11] VYSOCKÁ, A.—ŠPAKOVÁ, J.—DUSZA, J.—BALOG, M.—ŠAJGALÍK, P.: Kovove Mater., *45*, 2007, p. 223.

[12] ŠAJGALÍK, P.—DUSZA, J.: J. Europ. Ceram. Soc., *5*, 1989, p. 321.

[13] HVIZDOŠ, P.—RUDNAYOVÁ, E.—DUSZA, J.—BARINOV, S. M.—KRYLOV, A. V.: Kovove Mater., *34*, 1996, p. 133.

[14] LIU, S. Y.—CHEN, W.: Acta Mater., *44*, 1996, p. 2079.

[15] GONDÁR, E.—ROŠKO, M.—ZEMÁNKOVÁ, M.: Kovove Mater., *43*, 2005, p. 124.

[16] GONDÁR, E.—GÁBRIŠOVÁ, Z.—ROŠKO, M.—ZEMÁNKOVÁ, M.: Kovove Mater., *44*, 2006, p. 113.

[17] PULC, V.—GONDÁR, E.—ŠVEC, P.: In: Zborník z medzinárodnej konferencie pri príležitosti 40. výročia založenia Strojníckej fakulty TU v Košiciach. TU Košice 1992, p. 97.

[18] EVANS, A. G.—CHARLES, E. A.: J. Am. Ceram. Soc., *59*, 1976, p. 371.

[19] GONDÁR, E.—PULC, V.—ŠVEC, P.: Spôsob skúšania keramiky na odolnosť proti tepelnej únave. AO č. 284 53, 1.7.2005, Vestník ÚPV SR č. 7/2005.

[20] HLAVA, T.: Teplotná a napäťová analýza nitridu kremíka pri skúške odolnosti proti opakovaným tepelným rázom. [Dizertačná práca]. Bratislava, SjF STU 2005.